Modern Physics Letters B
(2023) 2350077 (10 pages)

DOI: 10.1142/S021798492350077X

Maximizing buckling load of metabeams via combinatorial optimization of microstructures

Xiangjun Chen and Meie Li*

State Key Laboratory for Mechanical Behavior of Materials,
School of Materials Science and Engineering, Xi'an Jiaotong University,
Xi'an 710049, P. R. China
**limeie@mail.xjtu.edu.cn*

Ning An

School of Aeronautics and Astronautics, Sichuan University,
Chengdu 610065, P. R. China

Jinxiong Zhou

State Key Laboratory for Strength and Vibration of Mechanical Structures
and School of Aerospace, Xi'an Jiaotong University,
Xi'an 710049, P. R. China

Received 10 November 2022
Revised 27 February 2023
Accepted 26 March 2023
Published 26 May 2023

Design of mechanical metamaterials is typically realized by repeating microstructured building blocks or unit cells. Microstructures of these unit cells can be identical, whereas individual design of each cell and various combinations of unit cells definitely offer more freedoms and possibilities for combinatorial design of metamaterials. Unfortunately, this combinatorial design problem is prohibitively challenging, if not impossible, due mainly to its huge number of combinatorial cases. This paper poses and addresses the combinatorial optimization of a metabeam, aiming at maximizing its critical buckling load. The problem was conceptualized and solved by combination of ML accelerated surrogate modeling and optimization algorithm, and buckling and post-buckling performance of the optimal design was validated by high-fidelity simulations and experiments. The efforts provide efficient tools for combinatorial design of mechanical metamaterials. We publicly share all the data and codes for implementation.

Keywords: Mechanical metamaterials; combinatorial optimization; metabeam; buckling; combinatorial design.

*Corresponding author.

1. Introduction

Mechanical metamaterials are rationally designed architected materials that exhibit unique mechanical properties not observed in nature. Design of mechanical metamaterials is typically realized by regularly repeating unit cell structures in two or three dimensions, such as porous materials consisting of networks of beams,[1–4] kirigami-inspired stretchable metastructures,[5–7] origami-inspired reconfigurable structures,[8–10] and architected cellular materials.[11–13]

A metabeam is a column with an array of microstructured voids or a conventional solid beam coupled with a set of spring-mass resonators, falling into the category of one-dimensional (1D) mechanical metamaterials. Metabeams can be designed to achieve some unique properties, such as discontinuous buckling,[14] band gap and nonreciprocal propagation of waves,[15–19] extreme frequency conversion,[20] and spanwise wing morphing.[21,22]

We are interested in the class of metabeams where a regular line of microstructured centered voids are introduced in a soft slender column, especially in their buckling behavior under compression. Buckling may trigger dramatic homogeneous and reversible pattern transformations in flexible mechanical metamaterials.[23] Pihler-Puzovic *et al.*[24] reported that a thin elastic column with a regular line of circular holes exhibits an internal buckling mode in which the circular holes are transformed into an array of mutually orthogonal ellipses and the column remains straight. Coulais *et al.*[14] uncovered the discontinuous buckling of metabeams. The metabeams were made from mechanical metamaterials, where a silicone rubber beam was patterned by a regular array of elliptical holes, and discontinuous buckling featured by negative post-buckling stiffness was reported. Meanwhile, in engineering problems, buckling is a failure mode characterized by a sudden failure of a structure subjected to high compressive stresses, which plays an important role in the design of beams with structural voids. Many optimization works have been devoted to improving the buckling load-carrying capability of metabeams. Nazir *et al.*[25] experimentally and numerically found that the critical buckling load increases with the increase of unit cell size while the total mass, void volume fraction, and column dimensions remain the same. Oliveri and Overvelde[26] proposed a gradient-free stochastic optimization algorithm to tackle the disjoint topology optimization problem of metabeams with maximum buckling load. Wang *et al.*[27] developed an optimization framework by taking yield and buckling strength as constraints to minimize the compliance of a Messerschmitt–Bolkow–Blohm (MBB) beam consisting of either body-centered cubic (BCC) and primitive cubic (PC) lattices.

All the metabeams mentioned above possess a regular array of holes or voids with the same hole or pore shape, i.e. they only exhibit 1D periodicity. We take inspiration from the design of 2D mechanical metamaterials by exploring the effect of pore shape on the nonlinear response of a square array of pores in an elastomeric matrix,[28] and in particular the combinatorial design of aperiodic mechanical metamaterials that exhibits spatially textured functionalities.[29] Different from metamaterials design

with a regular array of pores with the same shape throughout the metamaterials, we instead design a metabeam consisting of a line of microstructured voids with different pore shapes. We pose and address an intriguing problem of maximizing buckling load of a metabeam through combinatorial optimization of microstructured cells.

2. Modeling

Figure 1 shows the schematic of the problem considered in this study. The metabeam considered here is made from elastomeric 1D mechanical metamaterials consisting of a line of unit cells with microstructured pores. The number of unit cells n can be arbitrary for different designs, here, without loss of generality, we consider the case with $n = 10$, and each square cell has dimensions 10 mm $\times$ 10 mm. The bottom end of the beam is fixed and the metabeam is subjected to axial compression as shown in Fig. 1(a). Following Bertoldi,[28] the shape of the centered pore in each cell is assumed to be described by the following formula:

$$x_1 = r(\theta)\cos\theta, \quad x_2 = r(\theta)\sin\theta, \tag{1}$$

$$r(\theta) = \frac{L_0\sqrt{2\phi_0}}{\sqrt{\pi(2+a^2+b^2)}}[1+\cos(4\theta)+b\cos(8\theta)], \tag{2}$$

where x_1 and x_2 are the horizontal and vertical coordinates of the point on the hole boundary, respectively, and $0 \le \theta \le 2\pi$. a and b are the two parameters that control the shape of the hole. When both a and b are zero, a circular hole can be obtained, and changing the values of a and b can give a completely different pore shape. L_0 and ϕ_0 are the parameters that control the size of the hole. It is worth noting that keeping

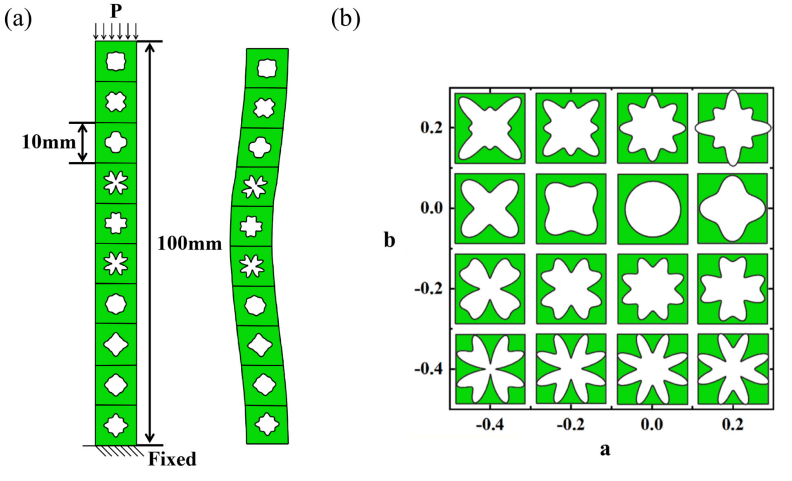

Fig. 1. (Color online) Schematics of the problem. (a) The geometry, loading and boundary conditions, and the first buckling mode of a slender metabeam consisting of 10 cells connected in series. (b) The microstructure of each cell is characterized by two parameters, a and b, and the combination of various a and b gives rise to the design phase diagram shown herein.

L_0 and ϕ_0 constants ensures the area of the hole a fixed value regardless the variations of a and b. In this study, L_0 was set to 6 mm and ϕ_0 to 0.5, which gives rise to a constant void area fraction of $f = 0.18$ (f being defined as the ratio between the void area and the total area). The design space of the various shapes of the pore is given in Fig. 1(b) for different combinations of a and b. To formulate the optimization problem and to parameterize the metabeam, a_i and $b_i (i = 1, 2, \ldots, 10)$ are used to denote a and b in Fig. 1(b) for the ith unit cell. The number of design variables is thus 20 in this case. We are concerned with the buckling load of the slender metabeam, and the classical global buckling is the first priority, which is dictated by the buckling load factor of the first mode λ_1. The mathematical description of the combinatorial optimization problem is now formulated as follows:

$$\begin{cases} \text{Find} : a_1, b_1, a_2, b_2, \ldots, a_{10}, b_{10}, \\ \text{Maximize} : \lambda_1, \\ \text{Subject to} : f_i = 0.18, \end{cases} \tag{3}$$

where a_1, b_1, …, a_{10}, b_{10} are the 20 design variables. f_i is the void volume fraction of the ith unit cell. As a constraint, f_i is fixed to be constant value 0.18 in all our following simulations.

The optimization problem formulated by Eq. (3) is a combinatorial optimization problem with maximum buckling load as objective and the optimal solution is obtained through combinations of pore shape parameters a_i and b_i. For each unit cell, the pore shape parameters a_i and b_i in Eq. (3) are both continuously varied from $[-0.4, 0.2]$. Thus, the design space for each cell is infinite in principle, and Fig. 1(b) only depicts the design space of one unit cell over a finite discrete values of a and b. For this type of optimization problem with very large design space and infinite number of freedoms to give different combination cases, design of experiment (DOE) and surrogate modeling are two crucial issues in practice.

In this study, we adopted our previously proposed surrogate model-based optimization framework[30] to solve the combinatorial optimization problem. The method consists of four steps as depicted in Fig. 2. The first step is DOE in which we sample the design space adopting the Latin hypercube technique and create a dataset. Second, the dataset from the first step is calculated using finite element model (FEM) to prepare for surrogate model building. Full automation of variable input, calculation and post-processing are conducted by writing Abaqus/python scripts. The third step uses the FEM database to build a surrogate model for rapidly predicting the critical buckling loads. Finally, this surrogate model is input into the commercial software Isight for optimization using the genetic algorithm NSGA-II.

Specifically, in order to ensure uniformly sample the 20 design variable parameters that make up the design space, we collected a total of 20,000 sets of data using the Latin hypercube sampling method (see the Supplementary Materials for details). Performing DOE is actually generating sampling space for all design variables. When DOE completes, it is then necessary to evaluate objective functions and constraints on all these sampling data. This can be conducted either by performing high-fidelity

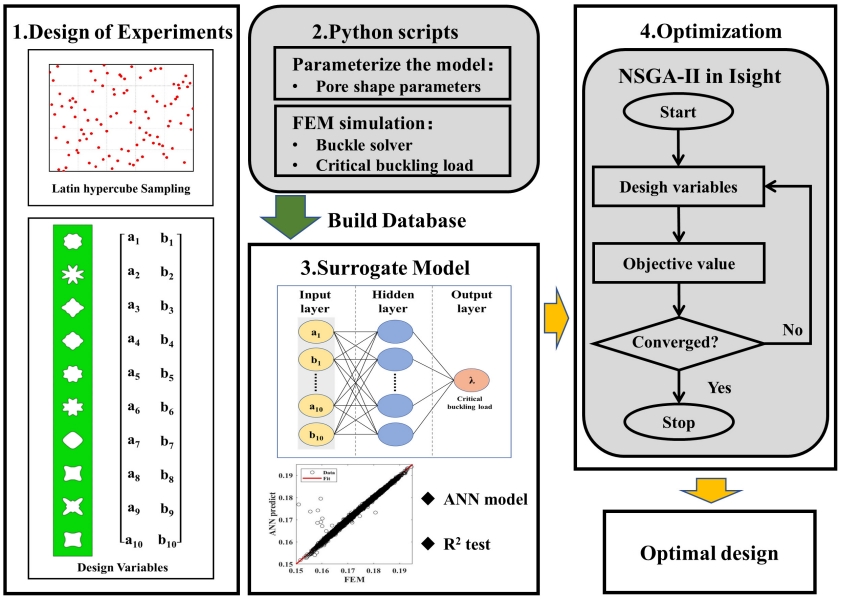

Fig. 2. (Color online) Workflow chart of the numerical strategy of maximizing buckling load of a metabeam via combinatorial optimization, which is realized through integration of DOE, parameterization of the metabeam, FEM simulation, surrogate modeling and genetic algorithm-based optimization.

FEM simulation for all sampling data, or, alternatively, performing FEM simulations only over a fraction of training data and then constructing a surrogate model to replace FEM simulation for the remaining sampling data. For large sampling datasets, this surrogate modeling is highly desirable. There are several well-established surrogate modeling techniques available, and we adopt the machine learning (ML)-based artificial neural network (ANN) model.

To start with, FEM simulations were performed to generate data for training and testing of the ML model. The commercial FEM code ABAQUS was used to deform the slender metabeam and to calculate its critical buckling force for each sampling design. 2D models were constructed using 6-node quadratic plane strain triangle elements (ABAQUS element type CPE6H) and the response of the elastomeric matrix is described by an incompressible Neo-Hookean material with initial shear modulus $\mu = 1.0\,\text{MPa}$. All degrees of freedom of the bottom edge were constrained, while the degrees of freedom of the top edge were coupled to a reference point where a unit compressive concentrated force was applied. The linear buckling problem was solved by an eigenvalue analysis step (*Buckle in ABAQUS). Python scripts were coded to parameterize the metabeam model, automate FEM simulations, and postprocess FEM results. An ANN-based surrogate model was generated using the FEM database on training data, and then compared with FEM results on testing data to guarantee the accuracy of the surrogate model. The trial-and-error approach was used to determine the structure of the ANN model. After tests, the structure of

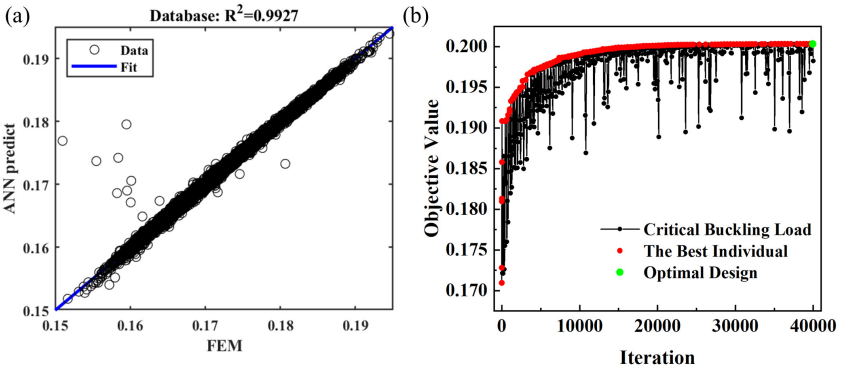

Fig. 3. (Color online) Performance of the surrogate modeling accelerated combinatorial optimization. (a) Correlation of ANN prediction versus FEM simulation, giving R^2 up to 0.9927. (b) Convergence history of the combinatorial optimization process.

the model is [20, 64, 1], which means that the neural network has 20 inputs, 1 output and one hidden layer with 64 neurons. The activation function was the Sigmoid function and the training algorithm was the Levenberg–Marquardt method. Once the surrogate model was validated, it was then integrated into the optimization software Isight 2020, and the combinatorial optimization problem was solved by a genetic algorithm (GA) NSGA-II in Isight. Thus during the whole optimization process, surrogate model is used in lieu of high-fidelity FEM simulations to evaluate objective functions, which speeds up optimization process and dramatically saves computation time and resources. The numerical scheme detailed above is illustrated schematically in Fig. 2, and it should be pointed that all the processes discussed previously were integrated in a seamless fashion. The procedure and the technique was previously validated by solving a shape optimization problem of deployable composite structures.[30] Figure 3(a) demonstrates the accuracy of the ANN surrogate model. A comparison is made between true FEM simulation and ANN prediction, and a R^2 correlation coefficient 0.9927 was achieved. Figure 3(b) plots the convergence history of objective function, which indicates that the optimal solution is obtained after nearly 40,000 iterations. The details of DOE, ANN parameters, FEM simulations can be found in Supplementary Materials. All the data and codes that support our findings are publicly shared via the link https://github.com/XJTU-Zhou-group/optimization-metabeam.

3. Results

Figure 4 presents and compares three combinations of microstructures. Figure 4 (a) shows the initial design randomly generated from design variables sampling, which yields a critical buckling load $\lambda_1 = 0.1703$. Fig. 4(b) presents a special case with all ten cells have identical circular holes with radius 2.40 mm, which gives $\lambda_1 = 0.1983$. Figure 4(c) shows the optimal microstructures combination, which

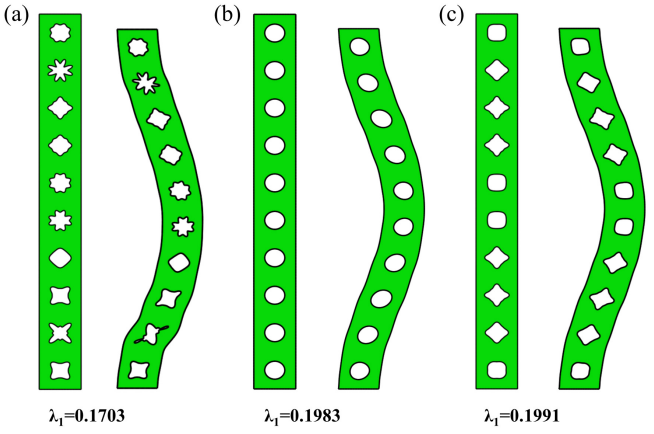

Fig. 4. (Color online) Combination of microstructures of a metabeam to maximize the critical buckling load. (a) A randomly generated initial design gives critical buckling load $\lambda_1 = 0.1703$; (b) A reference design with all pores being circular holes with the same radius. (c) The optimal design achieved via the proposed combinatorial optimization.

yields a critical buckling load $\lambda_1 = 0.1991$, slightly higher than the buckling load for identical circular holes.

The results in Fig. 4 numerically demonstrate the correctness of the proposed combinatorial optimization. We then performed experiment to further validate our idea, and the results are presented in Fig. 5. The metabeam sample was made of a soft glue material similar to silicone, and the production process was laminated. The metabeam was compressed vertically by SHIMADZU AGX-X universal testing machine (see Supplementary Movie). Two ends of the metabeam were clamped to fixtures as schematized in Fig. 5(a). Figure 5(b) plots the force-displacement curves for both initial design and optimal design. Force-displacement curves obtained from FEM were also included in Fig. 5(b) marked by the dotted lines. Note that in line with the experimental tests, a high-fidelity 3D FEM model was used to simulate the buckling and post-buckling behavior of the metabeam, and a nearly incompressible Neo-Hookean material model with experimentally measured shear modulus $\mu = 3.32\,\text{MPa}$ and buck modulus $K = 32.12\,\text{MPa}$ was taken. Although FEM simulations capture the critical buckling loads, marked by A and C for initial and optimal designs, respectively, discrepancy exists between simulation and experiment regarding the post-buckling behavior: Experiment gives an up-and-down curve while simulation yields a going up and then levelling off after the critical point. The reason for this discrepancy could be related to the geometric effects of testing specimens such as the misalignment of the microstructures due to fabrication process. Figure 5(c) gives snapshots of deformation of the metabeam taken from experiment and FEM. Various deformation states, A, B, C and D, are marked in both Figs. 5(b) and 5(c).

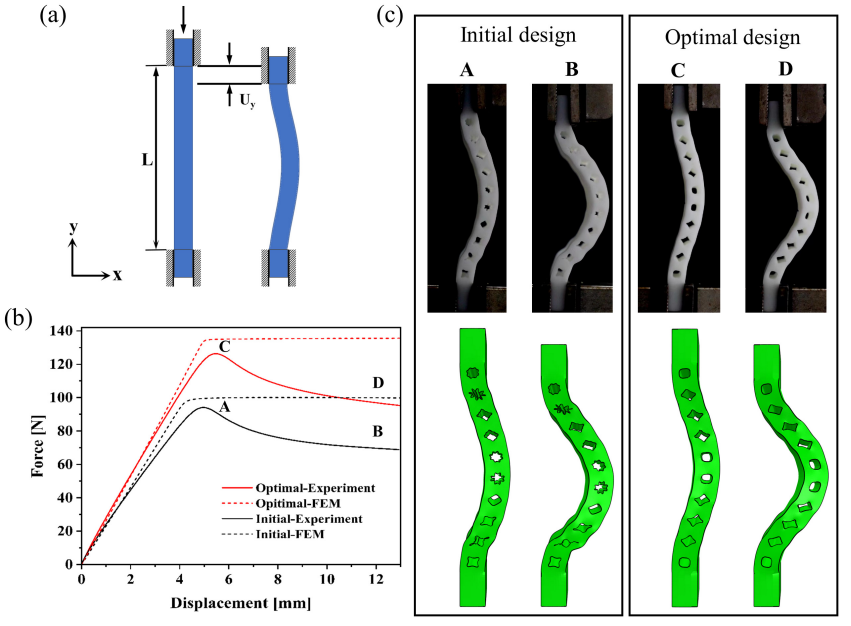

Fig. 5. (Color online) Experimental verification of the combinatorial design to maximize the buckling load of a metabeam. (a) Schematic of the experiment. (b) Force-displacement curves of the initial design (black lines) and the optimal design (red lines) obtained through experiment and FEM. (c) Snapshots of deformation of the metabeam taken from experiment(top) and simulation(bottom). *A*, *B*, *C* and *D* indicate various compression states and marked in the curves of (b).

4. Concluding Remarks

While early flexible mechanical metamaterials possess a regular array of voids with the same pore shape, increasingly complex combinatorial design of aperiodic mechanical metamaterials are being explored. This paper poses and addresses a combinatorial optimization problem for a metabeam with a line of microstructured pores. The controlling parameters for various shaped pores were chosen as design variables with maximizing compressive buckling load of the metabeam as objective, while the total mass, beam dimensions and void volume fraction remain unchanged. A combinatorial optimization problem was formulated and tackled by a surrogate modeling accelerated optimization strategy. The results reveal that, instead of having all identical pore shapes, the optimal design has a combination of various microstructures, holding a symmetric configuration with respect to the column midspan.

In summary, this paper demonstrates that a combination of different unit cell structures will probably outperform conventional mechanical metamaterials produced by simply repeating identical unit cells. We note that this work is limited to combinatorial optimization of 1D mechanical metabeams, and future studies are expected to explore the possibility of creating combinatorial designs in 2D and 3D

mechanical metamaterials. We hope the efforts will pave the way for combinatorial design of mechanical metamaterials. The flexibility and robustness of our method provide efficient tools for combinatorial design of mechanical metamaterial that would be impossible otherwise.

Acknowledgment

This research is supported by the Natural Science Foundation of China (Grant Nos. 11972277 and 12202295).

References

1. J. T. B. Overvelde, S. Shan and K. Bertoldi, *Adv. Mater.* **24**(17) (2012) 2337.
2. C. Coulais, A. Sabbadini, F. Vink and M. Van Hecke, *Nature* **561**(7724) (2018) 512.
3. Q. Xiong, T. G. Baychev and A. P. Jivkov, *J. Contam. Hydrol.* **192** (2016) 101.
4. X. Badiche, S. Forest, T. Guibert, Y. Bienvenu, J.-D. Bartout, P. Ienny, M. Croset and H. Bernet, *Mater. Sci. Eng. A* **289**(1–2) (2000) 276.
5. Y. Tang, G. Lin, S. Yang, Y. K. Yi, R. D. Kamien and J. Yin, *Adv. Mater.* **29**(v10) (2017) 1604262.
6. N. A. Alderete, N. Pathak and H. D. Espinosa, *NPJ Comput. Mater.* **8**(1) (2022) 191.
7. N. An, A. G. Domel, J. Zhou, A. Rafsanjani and K. Bertoldi, *Adv. Funct. Mater.* **30**(6) (2020) 1906711.
8. Z. Meng, M. Liu, H. Yan, G. M. Genin and C. Q. Chen, *Sci. Adv.* **8**(23) (2022) eabn5460.
9. G. Wen, G. Chen, K. Long, X. Wang, J. Liu and Y. M. Xie, *Mater. Des.* **212** (2021) 110203.
10. S. Babaee, J. T. B. Overvelde, E. R. Chen, V. Tournat and K. Bertoldi, *Sci. Adv.* **2**(11) (2016) e1601019.
11. M. Benedetti, A. Du Plessis, R. O. Ritchie, M. Dallago, S. M. J. Razavi and F. Berto, *Mater. Sci. Eng. R: Rep.* **144** (2021) 100606.
12. T. A. Schaedler and W. B. Carter, *Annu. Rev. Mater. Res.* **46** (2016) 187.
13. K. Bertoldi, *Annu. Rev. Mater. Res.* **47** (2017) 51.
14. C. Coulais, J. T. Overvelde, L. A. Lubbers, K. Bertoldi and M. Van Hecke, *Phys. Rev. Lett.* **115**(4) (2015) 044301.
15. M. Attarzadeh, J. Callanan and M. Nouh, *Phys. Rev. Appl.* **13**(2) (2020) 021001.
16. K. Wang, J. Zhou, H. Ouyang, L. Cheng and D. Xu, *Int. J. Mech. Sci.* **176** (2020) 105548.
17. H. Nassar, H. Chen, A. Norris and G. Huang, *Ext. Mech. Lett.* **15** (2017) 97.
18. A. Banerjee, *Phys. Lett. A* **388** (2021) 127057.
19. A. Banerjee and K. K. Bera, *Int. J. Mech. Sci.* **236** (2022) 107765.
20. M. Hwang and A. F. Arrieta, *Phys. Rev. Lett.* **126**(7) (2021) 073902.
21. D. M. Boston, F. R. Phillips, T. C. Henry and A. F. Arrieta, *Ext. Mech. Lett.* **53** (2022) 101706.
22. D. M. Boston, F. R. Phillips, T. Henry and A. F. Arrieta, Aeroelastic analysis of spanwise morphing wing with multistable honeycomb, in *AIAA SCITECH 2022 Forum* (2022), p. 0319.
23. K. Bertoldi, V. Vitelli, J. Christensen and M. Van Hecke, *Nature Rev. Mater.* **2**(11) (2017) 1.
24. D. Pihler-Puzović, A. Hazel and T. Mullin, *Soft Matter* **12**(34) (2016) 7112.
25. A. Nazir and J.-Y. Jeng, *Mater. Des.* **186** (2020) 108349.

26. G. Oliveri and J. T. Overvelde, *Adv. Funct. Mater.* **30**(12) (2020) 1909033.
27. X. Wang, L. Zhu, L. Sun and N. Li, *Mater. Des.* **206** (2021) 109746.
28. J. T. Overvelde and K. Bertoldi, *J. Mech. Phys. Solids* **64** (2014) 351.
29. C. Coulais, E. Teomy, K. De Reus, Y. Shokef and M. Van Hecke, *Nature* **535**(7613) (2016) 529.
30. H. Jin, Q. Jia, N. An, G. Zhao, X. Ma and J. Zhou, *AIAA J.* (2022) 1.